Article

Cell Reports

Emergence of Ebola Virus Escape Variants in Infected Nonhuman Primates Treated with the MB-003 Antibody Cocktail

Graphical Abstract

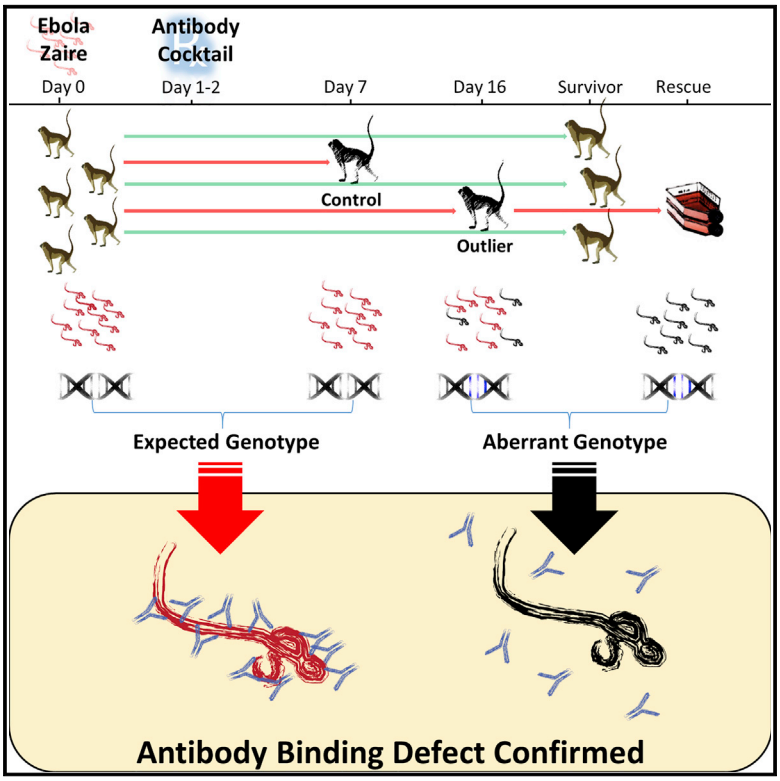

Authors

Jeffrey R. Kugelman, Johanny Kugelman-Tonos, Jason T. Ladner, ..., Gene G. Olinger, Mariano Sanchez-Lockhart, Gustavo F. Palacios

Correspondence

gustavo.f.palacios.ctr@mail.mil

In Brief

Ebola virus escape variants were discovered in infected non-human primates after treatment with the monoclonal antibody cocktail MB-003. Genome-based investigations revealed such mutants to rapidly emerge under selection pressure, suggesting that Ebola virus could evolve to become resistant to therapeutics under development for humans. These findings highlight the need for improved understanding of mutation emergence, the need to establish methods to clinically monitor the appearance of escape variants in real time, and the possible need for reformulation of passive immunotherapeutics.

Highlights

- Selection pressure by passive immunotherapeutics can cause rapid Ebola virus mutation
- Identifying sites susceptible to this selection pressure is a high priority
- Passive immunotherapeutics may have to be reformulated to prevent escape variants

Kugelman et al., 2015, Cell Reports *12*, 2111–2120
September 29, 2015 ©2015 The Authors
http://dx.doi.org/10.1016/j.celrep.2015.08.038

Cell Reports
Article

Emergence of Ebola Virus Escape Variants in Infected Nonhuman Primates Treated with the MB-003 Antibody Cocktail

Jeffrey R. Kugelman,[1,6] Johanny Kugelman-Tonos,[2,6] Jason T. Ladner,[1] James Pettit,[4] Carolyn M. Keeton,[1] Elyse R. Nagle,[1] Karla Y. Garcia,[1] Jeffrey W. Froude,[3] Ana I. Kuehne,[3] Jens H. Kuhn,[4] Sina Bavari,[2] Larry Zeitlin,[5] John M. Dye,[3] Gene G. Olinger,[4] Mariano Sanchez-Lockhart,[1] and Gustavo F. Palacios[1,*]

[1]Center for Genome Sciences
[2]Molecular and Translational Sciences Division
[3]Virology Division
United States Army Medical Research Institute of Infectious Diseases (USAMRIID), Fort Detrick, Frederick, MD 21702, USA
[4]Integrated Research Facility at Fort Detrick, National Institute of Allergy and Infectious Diseases, National Institutes of Health, Fort Detrick, Frederick, MD 21702, USA
[5]Mapp Biopharmaceutical, Inc., San Diego, CA 92121, USA
[6]Co-first author
*Correspondence: gustavo.f.palacios.ctr@mail.mil
http://dx.doi.org/10.1016/j.celrep.2015.08.038

SUMMARY

MB-003, a plant-derived monoclonal antibody cocktail used effectively in treatment of Ebola virus infection in non-human primates, was unable to protect two of six animals when initiated 1 or 2 days post-infection. We characterized a mechanism of viral escape in one of the animals, after observation of two clusters of genomic mutations that resulted in five nonsynonymous mutations in the monoclonal antibody target sites. These mutations were linked to a reduction in antibody binding and later confirmed to be present in a viral isolate that was not neutralized in vitro. Retrospective evaluation of a second independent study allowed the identification of a similar case. Four SNPs in previously identified positions were found in this second fatality, suggesting that genetic drift could be a potential cause for treatment failure. These findings highlight the importance selecting different target domains for each component of the cocktail to minimize the potential for viral escape.

INTRODUCTION

Ebolaviruses (Bundibugyo, Ebola, Reston, Sudan, and Taï Forest viruses) are endemic to Africa and Southeast Asia and cause severe febrile bleeding disorders leading to multi-organ failure in humans and/or nonhuman primates (NHPs) (Kuhn, 2008). The mean lethality of ebolavirus infections is extremely high (mean as of March 11, 2015: 41%) (WHO, 2015). Prior to the current sustained epidemic in Western Africa (Baize et al., 2014), caused by Ebola virus (EBOV), outbreaks have typically occurred only intermittently within localized areas (Kuhn, 2008). The current Ebola virus disease (EVD) outbreak is substantially larger (thousands rather than dozens or hundreds of cases), affecting mainly Guinea, Liberia, and Sierra Leone. People who were infected with EBOV in these areas have also traveled or been transported to Mali, Nigeria, Senegal, Germany, Spain, the United Kingdom, and the United States (WHO, 2014b). The situation in the Western Africa outbreak area and the risk of expansion to other countries prompted the World Health Organization to adopt emergency measures to contain the outbreak, such as supporting the testing of as yet unapproved medical countermeasures in the affected human population (WHO, 2014a).

At least four types of post-exposure therapeutics have been effective in reducing mortality in NHPs after EBOV inoculation. These include (1) small interfering RNA (siRNAs) (Geisbert et al., 2010), (2) phosphorodiamidate morpholino oligomers (PMOs) antisense strategies (Iversen et al., 2012; Warfield et al., 2006; Warren et al., 2010), (3) vesicular stomatitis Indiana virus (VSV)-based vaccines (Feldmann et al., 2007; Geisbert et al., 2008, 2009), and (4) passive immunotherapy (Olinger et al., 2012; Qiu et al., 2012a, 2013). One example of the latter is the monoclonal antibody (mAb) cocktail MB-003, a cocktail of three plant-derived monoclonal antibodies, designated c13C6, h-13F6, and c6D8. In rhesus monkeys, a benefit of 50%–100% survival was observed when MB-003 was administered within 24–72 hr after EBOV inoculation (Olinger et al., 2012). A study evaluating a different combination of mAbs called ZMAb (Public Health Agency of Canada), containing mAbs 1H3, 2G4, and 4G7, resulted in 100% survival when administered to the animals 24 hr after EBOV exposure, and 50% protection when administered after 48 hr (Qiu et al., 2012a). During the ongoing EVD outbreak in Western Africa, a third formulation, ZMAPP, containing mAbs c13C6, 2G4, and 4G7 (Qiu et al., 2014b; WHO, 2014b), has been administered to seven EBOV-infected patients. Five of them survived, but it is unclear whether survival was linked to the treatment (McCarthy, 2014). Moreover, due to the depletion of the stockpile of ZMAPP, previous

formulations are also being utilized for compassionate reasons (Penty and Benoit, 2014).

The basic mechanism of action of these therapeutic cocktails is the neutralization of viral replication through interaction of these mAbs with the EBOV glycoprotein ($GP_{1,2}$) (Bale et al., 2012; Lee and Saphire, 2009). $GP_{1,2}$ is responsible for Ebola virion attachment to its cognate host cell-surface receptor and subsequent fusion (Takada et al., 1997). $GP_{1,2}$ is located on the surface of the virion, is highly immunogenic, and is the main target of neutralizing antibodies (Bale et al., 2012; Lee et al., 2008; Olal et al., 2012; Wilson et al., 2000).

In a study that evaluated the efficacy of MB-003 as a post-exposure therapeutic for EBOV infection, two of the treated NHPs succumbed to infection (Olinger et al., 2012). To study the possible mechanisms of this partial MB-003 failure, we used a variety of genomic sequencing techniques to characterize the Ebola virus population present in the animals and to monitor the development of resistance to the therapy. The animal that succumbed at the expected time of death (11 days post-inoculation) for the infection did not show any significant changes in genomic diversity. However, the animal that died outside of the expected time (16 days post-inoculation) showed significant genomic changes. The derived viral genotypes were cloned into a plasmid transfection system and a phage display system to confirm the epitope disruption, thus linking the variants to an escape phenotype that appeared most likely in response to the mAb cocktail therapeutic. The resistant virus was isolated from the succumbed animal and characterized to demonstrate the mutant variant was infectious, capable of replication and able to also escape in vitro neutralization. Finally, retrospective analysis of a second independent study allowed the identification of a similar virus genotype in another NHP that also succumbed to infection on day 16, despite treatment with MB-003.

RESULTS

Viral Population Genomics

Viral populations from four different NHPs were characterized from study A (Table S1). Individual 5C succumbed on day 16 post-infection after therapeutic treatment with MB-003 (Olinger et al., 2012). Four blood samples were analyzed for this individual (days 6, 10, 14, 16 post-inoculation). Two blood samples were analyzed from a second MB-003-treated individual (NHP 3C, days 6 and 10) that succumbed at the expected time of death (11 days post-inoculation). Additionally, analysis was performed in two mock-treated individuals, as controls (NHP 4C and 8C, days 6 and 7 post-inoculation). Deep sequencing of the entire viral genome was performed for each sample to characterize the viral population and to compare with the diversity observed in the viral stock utilized for inoculation (methods previously described [Kugelman et al., 2012]). While the viral genomic populations remained relatively homogeneous and unchanged in the samples taken at days 6 and 10 for animal 5C (and in all samples obtained from 3C, 4C, and 8C), the resulting single nucleotide polymorphism (SNP) profile indicated the appearance of significant subclonal diversity by day 14 that increased at day 16. Nine changes >2% were observed, which clustered in two regions of the *GP* gene (positions 6854–6885 and 7221–7256; Figure S1). These regions overlap with the protein binding sites of the mAbs: c6D8: 7204–7252, h-13F6: 7240–7288, and c13C6: 6039–7134 (Table S2) (Wilson et al., 2000). mAbs c6D8 and h-13F6 are known to bind to linear epitopes, whereas c13C6 was found to bind to a conformational epitope in the GP_1 subunit of $GP_{1,2}$ (Wilson et al., 2000). One of the SNPs (position 6854) was an A to C transversion, the rest were A to G transitions. These SNPs led to five nonsynonymous changes, one of which (K272N) was in a structured region near the mucin-like domain within the full-length $GP_{1,2}$. The other nonsynonymous mutations (T283A, D397G, Q406R, and the pleomorphic position K395R/G/E) were located within the nearby mucin-like domain at the virion/host-cell interface; however, structural information for this region is not yet available.

We previously demonstrated that the ebolavirus genome displays significant plasticity while changing in vivo and in vitro replication states (Kugelman et al., 2012). A change in the glycoprotein (*GP*) gene-derived mRNA caused by co-transcriptional polymerase stuttering at a polyadenylyl site results in the most significant change and relates to the ratio of 7U/8U forms (8U is preferred in vitro, while the 7U genotype is quickly recovered once the cell-culture passaged virus is utilized to infect an NHP). A similar pattern was described previously in guinea pigs (Volchkova et al., 2011). The 7U/8U ratio is important as it will affect the proportion of full-length $GP_{1,2}$ (8U) to secreted variants of unknown function, sGP (7U) and rarely ssGP (6 and 9U), during infection. While we observed this classical pattern (quick reversion to the 7U genotype) in all control animals (4C and 8C), and the treated animal that succumbed 11 days post-infection (3C); the animal 5C from which we recovered the viral escape mutant only slowly reverted to the 7U genotype (20% 7U at day 6; 33% at day 10; 40% at day 14 and 97% at day 16).

Viral Haplotype Phasing

The two observed clusters of mutations are situated approximately 400 nt apart, which is too far for individual reads from the Illumina dataset to span. Therefore, we utilized long reads from the Pacific Biosciences platform to determine whether these mutations occurred on the same or on different RNA molecules. A summary of the observed haplotypes is provided in Table 1. A haplotype is reported if it was significantly detected in both replicates of a particular sample ($p \leq 0.05$). As expected from the Illumina data, only one significant haplotype was detected in the samples taken from animal 5C on days 6 and 10. Nine significant haplotypes were detected on day 14, which are estimated to range in frequency from 1.2%–63.7%, and 11 haplotypes were detected on day 16, with frequencies estimated to range from 1.7%–26.4%. The frequency of the wild-type (WT) genotype decreased over time, starting with the day 14 sample, and by day 16, only 17.5% of the population still contained the WT genotype at the nine focal positions. We were unable to resolve a single evolutionary trajectory due to the presence of several loops in the haplotype network (Figure 1). Given the animal was challenged with a high-dose intra-muscular inoculation (690 pfu/ml) (Olinger et al., 2012), it is most likely that these loops are the result of homoplasies (i.e., the same mutations occurring in multiple different lineages); however, this pattern could also result from recombination.

Table 1. SNP Phasing

	Genotype									Non-Synonymous					Day 6		Day 10		Day 14		Day 16		
															Pop (%)	± (%)	Pop (%)	±	Pop (%)	± (%)	Pop (%)	± (%)	
1	C	G	G	A	G	G	A	A	A	N	A	R	G						13.69	1.32	26.41	4.56	
2[a]	A	A	A	A	A	A	A	A	A	K	T	K	D	Q	98.71	1.29	100.00		63.73	3.14	17.47	0.16	WT
3	A	A	A	G	G	A	A	G	G			G		R					3.32	1.69	15.02	1.24	
4	A	A	A	A	G	G	A	A	A			R	G						5.35	0.50	14.67	1.81	
5	A	A	A	G	G	A	G	G	G			G		R					1.47	0.50	7.33	0.82	
6	A	A	A	A	G	A	A	A	A			R							1.84	0.04	2.92	0.77	
7	A	A	A	A	A	A	A	G	A					R							2.59	0.95	
8	C	G	G	A	A	A	A	A	A	N	A								2.16	0.48	2.59	0.93	
9	C	G	G	G	G	A	A	G	G	N	A	G		R							2.21	0.95	
10	C	G	G	A	G	A	A	A	A	N	A	R							1.22	0.12	1.76	0.32	
11	A	G	G	A	G	G	A	A	A		A	R	G								1.67	0.29	
12	C	A	A	A	A	A	A	A	A	N									3.52	0.71			
	6854	6857	6885	7221	7222	7228	7247	7255	7256	272	283	395[b]	397[b]	406[b]									

EBOV from an animal that succumbed to infection on day 16 was subjected to amplicon sequencing, spanning both sites of interest (*GP* gene positions 6854–7256) on the Pacific Biosciences RS, in duplicate. This table contains a listing of the haplotypes, non-synonymous changes, and the estimated percentage of population by day for each haplotype. Only haplotypes that were significantly detected ($p \leq 0.05$, binomial distribution) in both replicates are shown. Nucleotide references refer to genome positions based on reference sequence AY354458; amino acid positions refer to the position from the start site of the *GP* gene-encoded $GP_{1,2}$.

[a]The wild-type sequence from the EBOV stock is designated (WT in the last column) for reference.

[b]Residues located in the mucin-like domain.

Evaluation of the Effect of the Observed Changes on Antibody Binding

To investigate the biological effect of the observed changes, we expressed WT and modified EBOV $GP_{1,2}$ containing the nonsynonymous changes described in the haplotype analysis (mutants Δ1S1 [K272N, T283A], Δ2S1 [K395G, D397G, Q406R], Δ1-2S1 [K272N, T283A, K395G, D397G, Q406R]) in a transient eukaryotic expression system using HeLa cells. Mutant Δ1 contains all of the nonsynonymous changes observed within the first cluster of mutations (6854–6885), mutant Δ2 contains all of the nonsynonymous changes in the second cluster (7221–7256), and Δ1-2 includes the changes from both clusters. $GP_{1,2}$ expression was assessed by high-content imaging microscopy with a rabbit polyclonal EBOV-$GP_{1,2}$ antiserum (IBT Bioservices). A panel of four conformational monoclonal antibodies (including mAb KZ52, a "base" $GP_{1,2}$ binding antibody [Dias et al., 2011; Maruyama et al., 1999]), and the corresponding individual MB-003 mAbs (c6D8, c13C6, and h-13F6) were also assessed to address correct $GP_{1,2}$ folding and possible epitope disruption, respectively. The four mAbs that bind conformational epitopes recognized the wild-type or mutated $GP_{1,2}$ similarly, proving that the mutations added to $GP_{1,2}$ have no major effects on the overall $GP_{1,2}$ conformation and folding (Figure 2A). The quantitative high-content imaging analysis confirms that the amino acid changes introduced in the EBOV glycoprotein significantly disrupt non-competitive binding of the three monoclonal antibodies comprising MB-003 (Figure 2A). Changes to each region were sufficient to reduce binding efficiency as compared to WT across all mutants. Remarkably, changes introduced into the Δ1 region of $GP_{1,2}$, outside the known linear epitope for mAbs c6D8 and h-13F6, also disrupt binding; this is likely due to conformational changes in the $GP_{1,2}$ structure that do not affect the other four mAb antibodies tested. No localization changes for any of the mutant versions of $GP_{1,2}$ were seen in the microscopy analysis (Figure S2). The mAb c13C6 recognition site has been described as conformational and it has been unequivocally identified to react with sGP (Wilson et al., 2000). Intriguingly, the findings that mutations in both regions disrupt c13C6 binding suggests they are directly or indirectly involved in the c13C6 conformational epitope. Given the disordered nature of this region of the protein, we cannot speculate about the structural effects that might contribute to these changes in affinity. Additional work might be necessary to define the precise binding properties of this mAb, which is included not only in MB-003, but also in its successor, ZMAPP (Qiu et al., 2014b; WHO, 2014b).

Although these experiments indicate the loss of binding of the mAbs to the virus $GP_{1,2}$, and therefore suggest that the mutations observed are the result of positive selection imposed by the passive immunotherapy treatment, these experiments are non-competitive. To test the preference of the binding of the antibody in a mixed population, we developed a system based on phage display, in which we expressed the different haplotypes and used the monoclonal antibodies to competitively select from the expressing phages within the library. Phages displaying the WT sequence or peptides representing the haplotypes of Δ2 (K395R/G, D397G, Q406R) were panned against mAbs c6D8 and h-13F6. Resulting bound and unbound phage libraries were deep sequenced to provide differential expression data. Figure 2C depicts the enrichment or reduction of binding affinity to each mutant phage. All of the haplotypes tested affected the binding of h-13F6 or c6D8 to their known binding regions. Monoclonal antibody h-13F6 led to an average reduction of 94.3% ± 1.1% in enrichment compared to WT for variants containing Q406R, whereas changes occurring further upstream

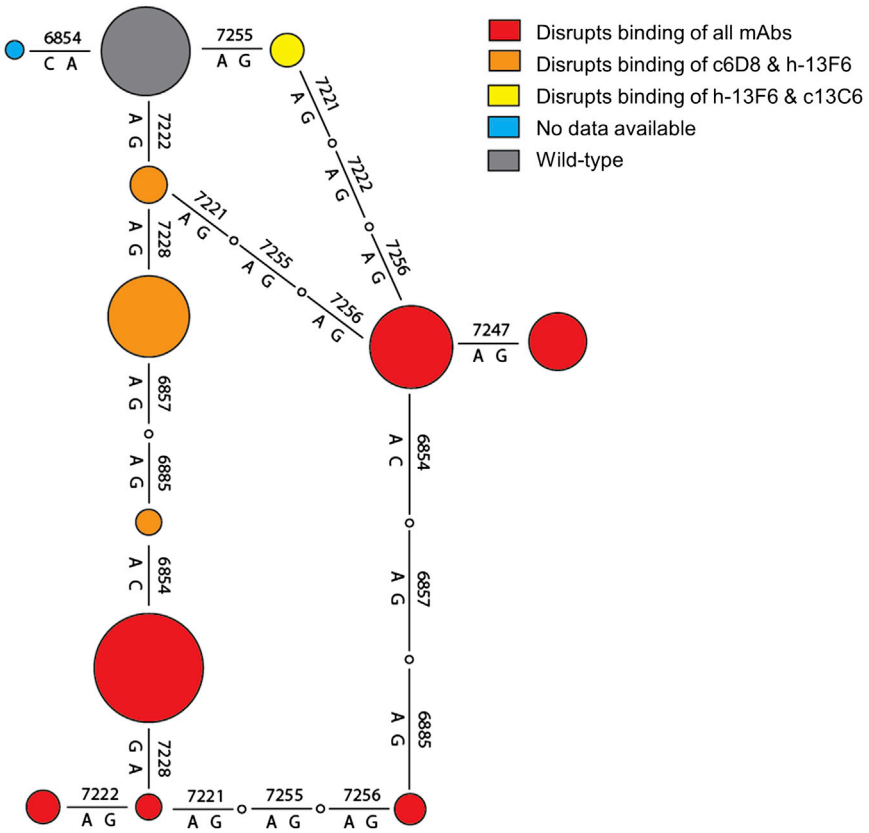

Figure 1. Haplotype Network

A haplotype network depicting the 12 EBOV haplotypes detected in the blood samples from individual 5C. Each line corresponds to a single genetic change. The colored circles represent detected haplotypes, and the white circles represent inferred haplotypes that were not detected. The size of each circle is relative to the estimated frequency of the haplotype on day 16 (except for the blue haplotype, which was only detected on day 14). The wild-type haplotype is shown in gray; the other haplotypes are colored based on their detected ability to disrupt the binding of the three therapeutic monoclonal antibodies (Figure 3).

of the published binding site led either to no change in abundance or modest, highly variable reductions (on average 18.2% ± 23.9% enrichment compared to WT). This result is expected since the mutation at Q406 is a key contact of 13F6 (Lee et al., 2008). Monoclonal antibody c6D8 led to a reduction of 97.3% ± 0.3% enrichment as compared to WT across mutations in the published binding region (Wilson et al., 2000), whereas the single Q406R mutation that lies downstream led to a 65.7% ± 10.4% reduction in enrichment compared to WT.

Recovery of Mutant Virus

In the original study evaluating MB-003, EBOV was not recovered from the samples collected from animal 5C on day 16 (Olinger et al., 2012). We repeated that isolation attempt with the goal of ensuring that the mutated virus was viable. We observed a cytopathic effect after two blind passages and 14 days of culture in Vero E6 cells (7 days per passage). EBOV was harvested and subjected to deep sequencing analysis. Table 2 summarizes the sequencing results covering the area of interest. The recovered EBOV population carried all five nonsynonymous mutations. The predominant haplotype (~79% frequency) matched the most abundant haplotype present at day 16 (haplotype 1 in Table 1). Only one additional nonsynonymous change was acquired during passaging (R409C), which indicated that these mutations do not dramatically impact fitness in vitro. Neither the pool of the mAbs that formed the cocktail nor two of the three individual mAbs neutralized the virus recovered from NHP 5C at day 16 or a plaque purified virus from the same stock (Figure 3). The same pool and each individual mAb (c13C6 or c6D8) reduced 80% of the wild-type EBOV stock plaques at a concentration of 12.5 or 25 μg/ml, respectively. Monoclonal antibody h-13F6 was not tested individually as it does not have in vitro neutralizing properties (Wilson et al., 2000).

Retrospective Evaluation of Treatment Failures

We were able to retrospectively identify two additional individuals that were also unsuccessfully treated with MB-003. One treated individual succumbed at day 11 p.i. (NHP10); the second succumbed at day 16 (NHP01). A mock-treated animal that succumbed on day 10 p.i. from the same study was also analyzed as a control (NHP04). All three NHPs were assayed for diversity in the region identified above (6800–7300 nt) using high-throughput amplicon sequencing. No significant sub-clonal diversity was detected in this region in NHP10 or NHP04. However, NHP01 (which succumbed later at day 16 p.i.) presented two sub-clonal clusters of diversity in this region by day 14 (Table 3). These clusters overlap with the clusters observed in animal 5C. In fact, four of the variant amino acid positions observed in animal 5C were also variable in NHP01 (though the exact same mutation was not observed in all cases, and one of the mutations [7255] was observed at a lower level). Two additional high-frequency sub-clonal nonsynonymous variant positions (6849 and 7263) were also identified. We introduced these mutations into $GP_{1,2}$ as described before (mutants Δ1S2 [G271R, K272I], Δ2S2 [K395E, D397G, Q406L, R409C], Δ1-2S2 [G271R, K272I, K395E, D397G, Q406L, R409C]). A quantitative high-content imaging analysis using this additional set of haplotypes confirms that the changes introduced in the EBOV glycoprotein significantly disrupt binding of MB-003 without affecting conformational antibody bindings or localization of $GP_{1,2}$ (Figures 2B and S3). Moreover, changes introduced into the Δ1 region of $GP_{1,2}$ disrupt binding of mAbs c6D8 and h-13F6, while changes introduced into the Δ2 region disrupt c13C6, confirming the results observed with animal 5C.

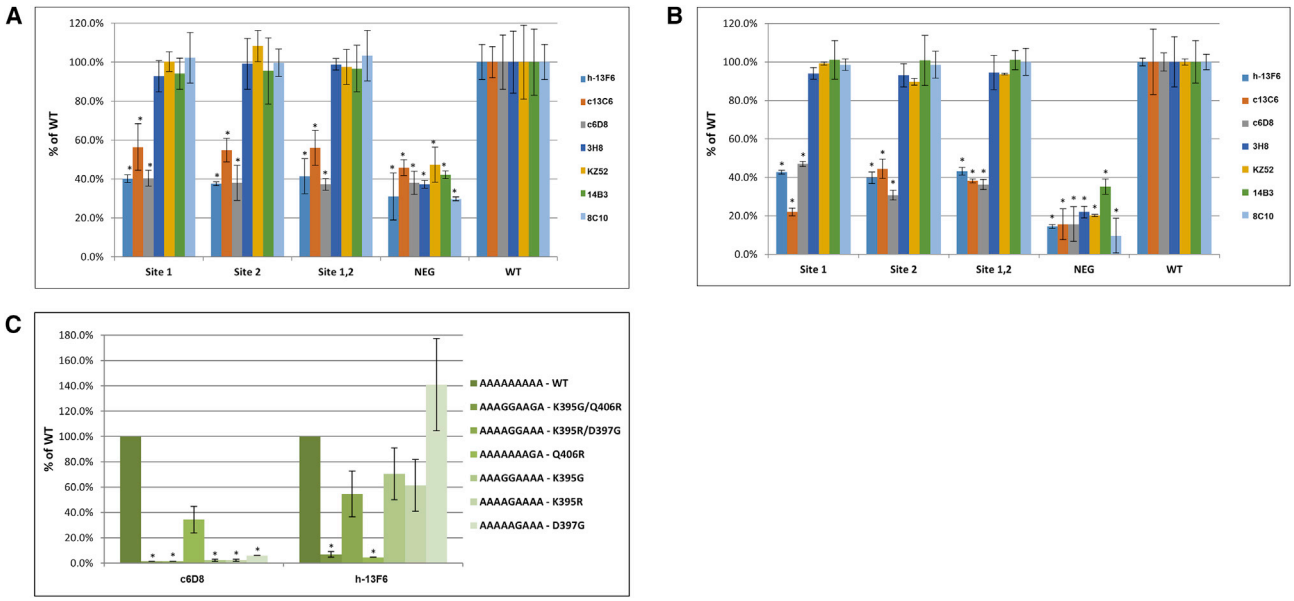

Figure 2. Binding Defect Analysis

High content imaging was performed on average >5,000 cells across 56 fields in quadruplicate experiments. Immunostaining average intensities are displayed for each mAb in the MB-003 cocktail, a polyclonal antibody as control and four conformational monoclonal antibodies as controls of proper folding. Error bars represent SD. Statistically significant ($p \leq 0.05$, Student's test) variation from WT is denoted by an asterisk. For full imagery set, see Figures S2 and S3. (A) 5C mutants. (B) NHP01 mutants. (C) Viral variant phage-capture competition. Oligonucleotides containing the sequence of the viral variants spanning the Δ2 site were synthesized and cloned into phages. The phages express the corresponding peptides and were enriched using the therapeutic mAbs c6D8 and h-13F6, in duplicate. Binding activities of the variant haplotypes were normalized against the wild-type for each antibody in duplicate experiments.

DISCUSSION

Our ability to follow the classical paths of research in the study of antiviral resistance mechanisms is severely impaired when therapeutics target select agents, such as EBOV. This is due to restrictions resulting from the policies regarding gain-of-function experiments and dual-use concerns that limit the ability to purposefully generate variants that escape medical countermeasures. Limitations related with gain-of-function experiments precluded us to perform in vivo studies with the viral escape mutant strain that could have measured its potential in vivo fitness. Thus, a thorough analysis of all treatment failures during experimentation in surrogate animal models becomes crucial to identify pathways of resistance. Due to the limited number of individuals who are tested in such studies owing to financial, logistic, and ethical concerns, the results can rarely be generalized. It is therefore highly desirable to perform viral population genomics studies and to monitor the appearance of mutants that might confer resistance to candidate therapeutics. Fortunately, currently existing capabilities for high-throughput, deep genomic sequencing facilitate this task.

The set of resistance-conferring mutations reported here appeared during the course of an EBOV infection in a rhesus monkey over 16 days and appear to be sufficient to overcome the protective capability of three promising mAbs that protected other individuals in the same study. These mutations were not observed in any other EBOV-RNA positive animal from the same study. The resulting EBOV variant appeared to be fit, although it was necessary to perform blind passages to recover it. The recovered viral population does not show any fitness costs in vitro, as demonstrated by normal growth curve and plaque size. The observed changes were not lost during further passage of the population, i.e., they seem to be genetically stable. The isolated virus was not neutralized in vitro by either of the two neutralizing mAbs (c6D8 and c13C6) or the cocktail, demonstrating conclusively that the virus was an escape mutant.

Strikingly, a very similar resistant genotype arose independently in a second NHP that succumbed at day 16 in a different study that included similar treatment and inoculation parameters. To date, 41 NHPs have been treated with MB-003 in six independent NHP animal experiments performed with the goals of evaluating proper dosage, antibody composition, and effective window of treatment. Seventeen (41.5% of total) succumbed despite treatment, two of which (11.8% of the deceased; 4.8% of total) succumbed on day 16, a time that is considered outside the normal time of death for the EVD NHP model. The virus populations in both of these cases developed similar mutations. While our studied sample number does not support statistical analysis among the treated individuals (n = 4), the resistance mutations only occurred in the two late time-to-death animals out of a total of seven non-survivors surveyed across two independent studies. The other five individuals all succumbed in the normal time-of-death windows (note: we only studied two of those animals, which exhibited a wild-type genotype at the time of death), linking time to death with the resistance mutations ($p = 0.0467$; Fisher's exact test). Given that resistance is not detected in all cases of treatment failure, additional unidentified factors remain that result in loss of efficacy. These causes of failure may include

Table 2. Population Genetics for the Recovered Virus from Animal 5C

Reference Position	Base	SNP	Frequency (%)	Codon	Feature	R4368[a] (%)
6854	A	c	92.2	K:AAA @ 272 → N:AAc	GP	0.05
6857	A	g	91.9	L:CTA @ 273 → L:CTg	GP	ND
6885	A	g	89.4	T:ACA @ 283 → A:gCA	GP	0.20
7222	A	g	99.7	K:AAA @ 395 → R:AgA	GP	0.27
7228	A	g	86.1	D:GAC @ 397 → G:GgC	GP	0.19
7255	A	g	48.3	Q:CAA @ 406 → R:CgA	GP	0.06

ND, not detected.

[a]Sequencing was also performed on the seed stock used to inoculate the NHPs for comparison, designated here as "R4368". None of the positions exceeded background error (±2% of population) though the potential exists that true variants exist below this threshold.

such issues as co-morbidity, genetic disorders, physical traits, or some as-yet-unknown factor. However, no co-morbidities were detected during physical health assessments prior to infection and/or treatment, as well as, continuous monitoring of symptoms.

None of the mutations reported here have been identified previously in other natural EBOV isolates. Even though Ebola virus genomic sequences are remarkably conserved over time, suggesting intra-host purifying selection (Carroll et al., 2013; Suzuki and Gojobori, 1997), filoviruses mutate with roughly the same frequency as most other mononegaviruses. For instance, the number of nucleotide differences between an EBOV isolate of the current, 2014, outbreak in Guinea (KJ660346), Ebola virus/H.sapiens-tc/COD/1976/Yambuku-Mayinga (NC_002549) isolated 40 years ago, and Ebola virus Ebola virus/H.sapiens-tc/COD/1995/Kikwit-9510621 (AY354458) isolated 20 years ago, are 586 and 537 out of roughly 19,000 nucleotides (~3%), respectively. In that context, the speed at which EBOV populations can change when faced with strong selective pressures, as presented here, is remarkable. This result highlights the extreme care that needs to be maintained in the administration of virion-targeted therapeutics for dangerous pathogens under emergency use limitations. Our observations emphasize the need to control the conditions during which viral targeted therapeutics are administered to protect the efficacy of the treatments. Isolation must be maintained to ensure that if viral variants are generated during treatment they are limited and end with the current infection.

Our data indicate that the MB-003 cocktail may not be ideal for treatment of human EBOV infections as the targets of the individual antibody components are too closely related. Two amino acid mutations (K395G and Q406R) were enough to disrupt the binding of the three monoclonal antibodies present in MB-003. The formulation has since been changed by including mAbs from the ZMAb cocktail that target different areas of EBOV $GP_{1,2}$, thus theoretically diminishing the likelihood of viral escape (Qiu et al., 2011, 2012b). Indeed, ZMapp has now been given to 24 NHPs with treatment initiation from 3 to 5 days post-infection, and no escape mutants have been observed to date (Qiu et al., 2014a; WHO, 2014a). Nevertheless, given the shortage of ZMapp antibody cocktail that resulted in the utilization in humans of earlier formulations, it is recommended that all cases that receive this type of treatment are closely monitored to detect the appearance of escape variants. Despite the fact that the cocktail approach is attempting to mimic the multidrug (e.g., in comparison with monotherapy treatment) paradigm of drug therapy that was very successful for HIV treatment, our results appear to indicate that a head-to-head comparison to compare rates of resistance generation between small molecules and antibody cocktails might be warranted. Moreover, the unexpected observation that mutations outside the mapped epitopes of some of these antibodies would nonetheless abrogate antibody binding is significant. It cannot then be assumed that a mutation distal from the footprint of the antibody would not affect the antibody therapeutic. Efficacy of antibody based therapeutics would need to be experimentally verified with each permutation of a naturally evolving virus.

Our findings highlight several concepts that are critical to EBOV-targeted therapeutic development: (1) viral mutation under selection pressure can occur extremely rapidly (as compared to the observed acquisition of mutations over several decades of evolution of EBOV would suggest); (2) studies to elucidate the most common mutations that confer phenotypic resistance are of high priority; (3) methods for clinically monitoring the appearance of resistant variants need to be established; (4) for passive immunotherapy treatments, reformulation may be required to overcome very rare events; and (5) vaccines, which instead induce a polyclonal response, will surely avoid the generation of resistance more effectively than sequence-based therapeutics; (6) techniques for exploring the EBOV and host immunogenic fitness landscape without violating dual-use and gain-of-function restrictions are urgently needed.

EXPERIMENTAL PROCEDURES

Post-Exposure Studies

The study design, specific reagent development, and exposure material were reported previously (Olinger et al., 2012). In brief, the exposure stock of Ebola virus (EBOV) *H.sapiens*-tc/COD/1995/Kikwit-9510621 (*Filoviridae*: *Ebolavirus*: *Zaire ebolavirus*; GenBank AY354458) was prepared at the US Army Medical Research Institute of Infectious Diseases (USAMRIID) from virus originally isolated from an infected patient during the 1995 EVD outbreak in Kikwit, Zaire. The mAbs (c13C6, h-13F6, and c6D8) that comprise MB-003 were produced via transient expression in the plant system ΔXTFT *Nicotina benthamiana* and mixed in equal amounts for treatment (16.7 mg/kg/mAb). Verification of target dose and viremia was conducted with an agarose-based plaque assay. Rhesus monkeys (*Macaca mulatta*) were inoculated intramuscularly with a target dose of 1,000 pfu/ml and then treated 24 hr (n = 3) or 48 hr post-infection (p.i.) (n = 3) following the schedule at day 1, 5, 8, and 10 (24 hr) or 2, 6, 8, and 10 (48 hr). The actual dose determined by plaque titration was 690 pfu/ml. The mAb control

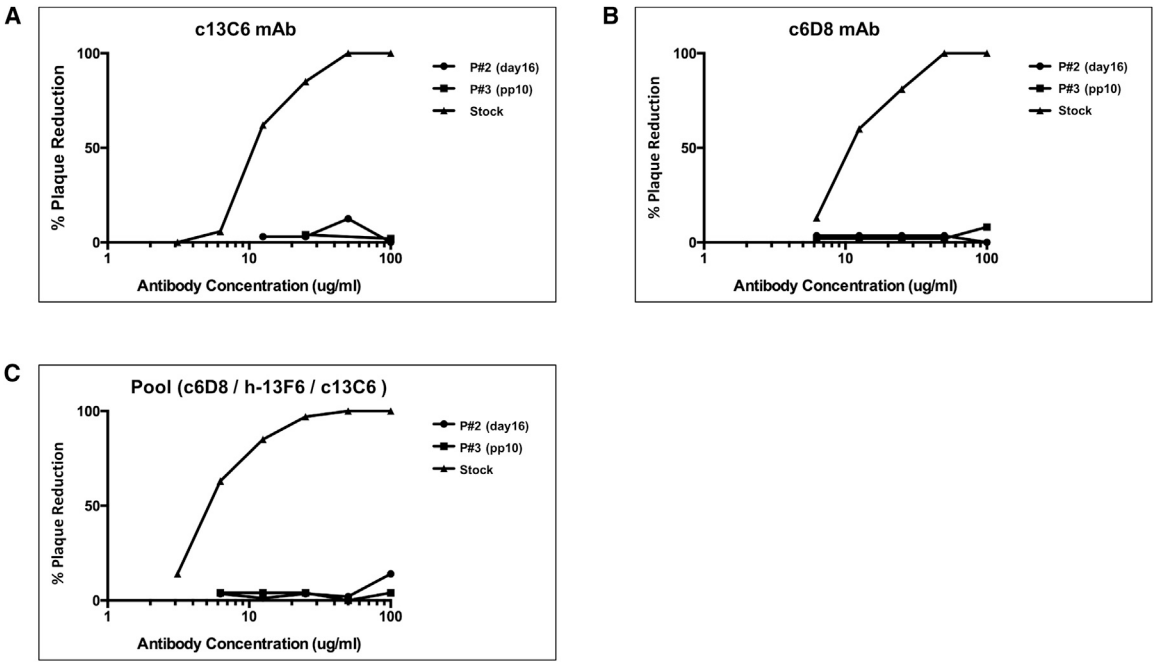

Figure 3. Neutralizing Antibody Assays

Viral plaques observed after 7 days p.i. in the presence 2-fold dilutions of the individual mAbs (A and B) and the MB-003 cocktail (C) were quantified for the seed stock used to inoculate the NHPs, the passage 2 of the 5C day 16 sera, and a plaque pick virus isolated from the passage 2. No differences in the growth curve shape or in the resulting plaque size were observed among the three viruses tested.

(n = 1; irrelevant target) was paired with the 24-hr group, and the PBS control (n = 1) was paired with the 48-hr group. For this study, blood samples were taken on days 2, 6, 10, 14, and 16 from a rhesus monkey that succumbed to EBOV infection on day 16 despite treatment 48 hr p.i. Blood samples were also taken from two control animals on days 6 and 7. For each sample, 0.25 ml blood were mixed with 0.75 ml TRIzol LS (Invitrogen) for serum virus inactivation. RNeasy kits (QIAGEN) were used for RNA extraction.

The second unpublished study (G.G.O. and J.M.D., unpublished data) followed similar exposure methods (Olinger et al., 2012). EBOV was also administered intramuscularly, and the NHPs were treated with MB-003 (or PBS as control) at 16.7 mg/kg/mAb at 24 hr p.i. Blood samples obtained on days 6, 9, or 10, and day 14 and 16 (for the late time-of-death NHPs) were available for analysis.

Virus Isolation from Plasma of NHP 5C, Day 16 Post-Infection with EBOV

EBOV was not recovered by the standard plaque assay method used for the isolation of EBOV. Serial passages in Vero cell monolayers were needed to isolate the virus. Briefly, a T25 with a Vero E6 confluent monolayer was inoculated with 200 μl of plasma from NHP057, day 16. After adsorption for 1 hr at 37°C, 5% CO_2, 80% H, 5 ml of growth media (EMEM [1×] with L glutamine and 1% NEAA, plus 5% heat inactivated FBS) was added to the monolayer. One T25 infected with 200 μl of EBOV and one T25 uninfected monolayer were used as controls. All monolayers were incubated at 37°C, 5% CO_2, and 80% H for 7 days and were daily observed for cytopathic effect (CPE). At day 7, 200 μl of supernatants from each T25 was transferred to fresh Vero E6 monolayers, and the monolayers were observed for another 7 days.

Virus Titration and Plaque Picking

The titer of 5C plasma day 16, Vero P2 was determined by the standard plaque assay method for filovirus (1×10^6 pfu/ml); 21 plaques were picked and amplified in Vero cell monolayers.

Animal Use Statement

Research was conducted under a protocol approved by an Institutional Animal Care and Use Committee (IACUC) in compliance with the Animal Welfare Act, PHS Policy, and other US federal statutes and regulations relating to animals and experiments involving animals. The facility in which this research was conducted (USAMRIID) is accredited by the Association for Assessment and Accreditation of Laboratory Animal Care, International (AAALAC) and adheres to principles stated in the Guide for the Care and Use of Laboratory Animals, National Research Council, 2011. The USAMRIID IACUC approved these studies.

Rhesus monkeys were individually housed in stainless steel cages and were provided food and water ad libitum. Animal rooms were maintained on a 12-hr-light/dark cycle and equipped with toy and fruit environmental enrichments. Animals were monitored at least twice daily for signs of distress. Buprenorphine was administered to animals having clinical signs of discomfort, and meloxicam was administered to animals with elevated body temperature. Euthanasia was performed to minimize pain and distress by intravenous administration of sodium pentobarbital.

Dual-Use Statement

Research was conducted under an IACUC-approved protocol in compliance with the Animal Welfare Act, Public Health Service Policy and other federal statutes and regulations relating to animals and experiments involving animals. The facility where this research was conducted is accredited by the Association for Assessment and Accreditation of Laboratory Animal Care International and adheres to principles stated in the 8th Edition of the Guide for the Care and Use of Laboratory Animals, National Research Council, 2011.

Research has been reviewed for compliance with dual-use guidelines and approved for publication by the USAMRIID Institute Biosafety Committee (IBC) and the Operational Security office.

Sequencing

Population Genomics Studies

cDNA synthesis was performed using Invitrogen's Superscript III First-Strand Synthesis System. cDNA was amplified with Phusion Hot Start Flex DNA Polymerase (New England Biolabs) using overlapping 1,500-kb amplicons (primer information available upon request). After pooling and purification with AMPure XP Reagent (Beckman Coulter), PCR products were fragmented

Table 3. Population Genetics for the Recovered Virus from Animal NHP01

Reference Position	Base	SNP	Frequency (%)	Codon	Feature
6849	G	C	21.85	G:GGA @ 271 → R:aGA	GP
6853	A	T	49.14	K:AAA @ 272 → I:AtA	GP
6885	A	g	ND	T:ACA @ 283 → A:gCA	GP
7221	A	g	2.20	K:AAA @ 395 → E:gAA	GP
7228	A	g	17.53	D:GAC @ 397 → G:GgC	GP
7255	A	g	0.49	Q:CAA @ 406 → L:CtA	GP
7263	C	t	40.90	R:CGC @ 409 → C:tGC	GP

ND, not detected.

using the Covaris S2 instrument (Covaris). Libraries were prepared with the Illumina TruSeq DNA Sample Preparation kit (Illumina) on the Caliper SciCloneG3 Liquid Handling Station (PerkinElmer). After measurement by real-time PCR with the KAPA qPCR Kit (Kapa Biosystems), libraries were diluted to 10 nM. Cluster amplification was performed on the Illumina cBot, and libraries were sequenced on the Illumina HiSeq 2500 using the 76 bp paired-end format (Kugelman et al., 2012).

Haplotype Sequencing Studies

cDNA was used as a template to generate a 1,500-bp amplicon spanning the EBOV *GP* gene positions 6490–7933 using touchdown PCR. Amplicons were purified using QIAGEN MinElute columns, and amplicon quality and concentration was measured with the Agilent 2100 Bioanalyzer. For sequencing on the PacBio RS II instrument, 2-kb libraries were generated and processed using the SMRTbell Template Prep Kit 1.0, the DNA/Polymerase Binding Kit P4, and the DNA Sequencing Reagent 2.0 (Pacific Biosciences). Two replicate amplicons were generated for each sample, and each replicate was sequenced on two SMRT cells.

Phage Sequencing

Phages recovered in the unbound and bound fraction were amplified by PCR using specific primers flanking the cloned oligos on the T7 phages. PCR amplification was performed with a denaturing step of 94°C for 3 min, 32 cycles of 94°C for 20 s (denature)/60°C for 20 s (annealing)/72°C for 30 s (extension), and a final extension step of 72°C for 10 min. Amplicons were recovered, cleaned using the QIAquick PCR purification kit (QIAGEN) and prepared for sequencing on the Illumina MiSeq. Sequencing libraries were run utilizing a 500 cycle kit (2 × 250 bp).

Analysis

Population Genomics Alignments

Viral assemblies were completed in DNAStar Lasergene nGen. Amplification primer removal, quality trimming, and trim-to-mer were performed on reads with a minimum similarity to the reference of 93% (four-base mismatch). SNPs at positions with fewer than 200 read depth were removed from the analysis. A consensus change is defined here as a change relative to the deposited EBOV sequence (GenBank AY354458) present in ≥50% of the population. Below that threshold, SNPs were considered sub-clonal substitutions and part of a minority subpopulation of the virus. Only SNPs present in the population above the 2% threshold are presented in this report.

Haplotype Analysis

Custom scripts were used to identify multilocus haplotypes using the PacBio sequences. To reduce error rates, circular consensus sequences (CCSs) were used with a minimum quality cutoff of 90 and a minimum number of full passes of 2. BLASR v.1.3.1 (Chaisson and Tesler, 2012) was used to align the CCS reads to the EBOV reference with N's substituted for the reference bases at the nine positions of interest (to minimize alignment bias; Carneiro et al., 2012). Reads were only utilized to infer haplotypes if a non-gapped alignment was achieved at all nine bases of interest. The binomial distribution was used to calculate the significance of each haplotype (i.e., likelihood that the haplotype was seen more often than would be expected by chance). The utilized error rate, 0.005, was calculated based on 100 simulated datasets (PBSIM with default parameters; Ono et al., 2013), which each included nine randomly selected variable sites, one primary haplotype (95% frequency), and five minor haplotypes (1% each). This error rate resulted in a precision of 0.998 (only one false-positive haplotype in all 100 simulations) and a recall of 1. Through repeated simulations it is clear that false-positives (FPs) are most likely to occur when one haplotype dominates the population (FPs are typically one base different from the dominant haplotype); therefore, the error rate chosen from these simulations is expected to be conservative for many real datasets. For each sample, the Bonferroni correction was used to control for multiple tests (# tests = # of detected haplotypes). A haplotype network was created using HapStar (Excoffier and Lischer, 2010; Teacher and Griffiths, 2011) to visual the relationships among the detected haplotypes.

Mutagenesis and Transient Expression

Transient Transfection

For transfection, HeLa cells were used at a confluence of 60%–80% plated in 96-well plates (Greiner Bio-one catalog no. 655090). cDNA from the respective constructs (plasmids expressing EBOV wild-type $GP_{1,2}$ [wtGP]) and mutants Δ1S1 (K272N, T283A), Δ2S1 (K395G, D397G, Q406R), or Δ1-2S1 (K272N, T283A, K395G, D397G, Q406R) (set 1) and Δ1S2 (G271R, *K272I*, T283A), Δ2S2 (K395G, D397G, Q406R, *R409C*), or Δ1-2S2 (G271R, *K272I*, T283A, K395G, D397G, Q406R, R409C) (set 2; underlined, additional mutation position; in italic, type of amino acid change) were prepared in serum-free DMEM. A mixture of 1 μl Lipofectamine 2000 in 24 μl serum-free DMEM and 25 μl of diluted plasmid (for a final volume of 50 μl, 300 ng of cDNA) per sample was incubated at room temperature for 20 min and then added to the cells and incubated for 6 hr at 37°C. Transfected cells were later washed with maintenance media (DMEM with 10% FBS) and incubated for 24 hr to allow $GP_{1,2}$ expression. Cells were washed with PBS and lysed with Pierce IP Lysis buffer.

High Content Imaging

Transfected cells were fixed with ice-cold methanol (−20°C) for 15 min at 4°C and permeabilized using 0.1% Triton-x 100 (Sigma-Aldrich, X-1005ML) for 10 min at room temperature. The cells were then washed twice with PBS and blocked with a solution containing 3% BSA (Fraction V) in PBS for 1 hr at room temperature. EBOV $GP_{1,2}$ was detected using the mouse monoclonal antibodies c6D8, c13C6, or h-13F6, human monoclonal antibody KZ52, mouse conformational monoclonal antibodies 3H8, 14B3, and 8C10, and the rabbit polyclonal antibody (IBT Bioservices, 0301-015) at a concentration of 1 μg/ml. Primary antibodies were diluted in 3% BSA and 100 μl added to each well for 1 hr. The cells were then washed three times with 0.1% PBS-T. The secondary antibody was added to each well at a concentration of 500 ng/ml (Alexa Fluor 488 for mouse monoclonal antibodies, Alexa Fluor 488 for human monoclonal antibody, and Alexa Fluor 555 for rabbit polyclonal antibody), incubated for 1 hr in the dark, and then the cells were washed three times with 0.1% PBS-T. The cell nuclei were stained with 1 ng/ml of Hoechst 33342 stain, and the plasma membranes were stained with 5 ng/ml of Cell Mask Deep Red. High content data were acquired and analyzed on the Operetta (PerkinElmer) high-throughput, wide-field fluorescence microscope reader (PerkinElmer) using the non-confocal setting with a 20× objective. On the operetta, images in the Blue (Hoechst 33342), Green (GFP or Alexa 488), DsRed (RFP 554), and Far Red (Cell Mask Deep Red) channels were sequentially acquired by a single charged-coupled device (CCD) camera. For each field of acquisition (63 fields were analyzed per well), a single imaging plane was automatically set by using an infrared laser based autofocus unit. The excitation light was provided using a 300 W Xenon lamp and images were acquired using a 20× long working distance objective. Image analysis was performed using the Harmony 3.0 software package (PerkinElmer).

Phage Display Competition

Oligonucleotides, encoding 28-mer peptides (WT: "THNTPVYKLDISEATQVE QHHRRTDNDS"), were designed to express epitopes from either wild-type $GP_{1,2}$ or the mutations observed in the viral population genetics study. Oligonucleotides were commercially printed (Eurofins Genomics) and cloned into the phage display plasmid (T7Select, EMD-Millipore) following the manufacturer's protocols. Monoclonal antibodies were coated at 10 μg/ml on 24-well plates in triplicates and incubated for 16 hr at 4°C. mAb dilutions were washed with 0.1 N NaHCO3 buffer (pH 8.6), and plate wells were blocked with 500 μl

10% BSA solution for 2 hr at 22°C. Blocking solution was removed from wells and plates were washed twice. 400 μl of the phage library was added per well,and plates were incubated 16 hr at 4°C. The unbound phage fraction was collected from the well and stored at 4°C. Plates were washed four times with TBS + 0.05% Tween 20. In the last two washed, plates were incubated for 20 min at 22°C before removal of the washing buffer. Bound phage fraction was collected from the wells after the fourth wash. Both fractions were stored at −20°C until sequencing.

Paired end reads produced on the Illumina MiSeq 2 × 250-bp kit were produced for the analysis. The reads were aligned read 1 to read 2 using the local aligner BLAST software from NCBI. The alignments were then used to correct sequencing errors. SNPs occurring only in one read were removed based on proximity to the 5′ end. Base calls near the 5′ end of the read were maintained. N's were discarded and the base from the opposing read was used. Tags used in the cloning process were used to determine the limits of the insert and the tags, and any Illumina adaptor sequences were trimmed. Reads that failed to be covered by both reads across the entire insert were removed as sequencing errors. The corrected reads were then compared to the original library design for categorization.

Neutralizing Antibody Assays

Two-fold dilutions of c13C6, c6D8, and h-13F6 or an equal combination of the three ranging from 3.12 μg/ml to 100 μg/ml were first incubated with 80 p.f.u. of EBOV at 37°C for 1 hr with or without complement, transferred to Vero E6 cells, and incubated at 37°C for 1 hr. After adsorption, monolayers were overlaid with a 1:1 mixture of EBME, 10% FBS, 1% penicillin streptomycin (10,000 U/ml), and 1% agarose. Plates were incubated for 7 days at 37°C, 5% CO_2, 80% humidity. A second overlay of 1:1 EBME and 1% agarose plus 5% neutral red was added, and plaques were counted 24–48 hr later. Titers were calculated when observing an 80% plaque reduction compared with the test control. Wild-type virus, the passage 2 of a virus recovered from the 5C animal at day 16, and a subsequently obtained plaque purified virus were used for neutralization experiments.

ACCESSION NUMBERS

The accession numbers for the NHP01, 4C D06, 4C D07, 5C D06, 5C D10, 5C D14, 5C D16, and 5C D16 rescue viral sequence alignments reported in this paper are BioSample: SAMN0312243, SAMN0312241, SAMN0312242, SAMN0312235, SAMN0312237, SAMN0312238, SAMN0312239, and SAMN0312240. The accession numbers for the 5C D06. 5C D10, 5C D14, and 5C D16 circular consensus sequence data reported in this paper are BioSample: SAMN0312244, SAMN0312245, SAMN0312246, and SAMN0312247.

SUPPLEMENTAL INFORMATION

Supplemental Information includes three figures and two tables and can be found with this article online at http://dx.doi.org/10.1016/j.celrep.2015.08.038.

AUTHOR CONTRIBUTIONS

S.B., J.M.D., G.G.O., L.Z., M.S.-L., and G.F.P. conducted the study design. J.R.K., J.K.-T., J.P., C.M.K., E.R.N., K.Y.G., J.W.F., and A.I.K. conducted the experimentation. J.R.K., J.K.-T., J.L., J.H.K., S.B., J.M.D., G.G.O., L.Z., M.S.-L., and G.F.P. conducted the Data Analysis and Data Interpretation. J.R.K., J.K.-T., J.T.L., J.H.K., S.B., J.M.D., G.G.O, L.Z., M.S.-L., and G.F.P. performed the writing.

CONFLICTS OF INTEREST

L.Z. is an owner of Mapp Biopharmaceutical, Inc.

ACKNOWLEDGMENTS

The authors thank Dr. W. Ian Lipkin for critical review of this manuscript, Dr. Krishna Kota for advice on the high content imaging systems used in the work, and the USAMRIID technicians: Guido Pelaez and Sarah Becker in the USAMRIID Molecular and Translational Sciences Division. This work was supported by Defense Threat Reduction Agency. The content of this publication does not necessarily reflect the views or policies of the US Department of the Army, the US Department of Defense, or the US Department of Health and Human Services or of the institutions and companies affiliated with the authors. J.H.K. performed this work as an employee of Tunnell Government Services, Inc., and G.G.O. and J.P. as employees of MRI Global, both subcontractors to Battelle Memorial Institute under its prime contract with NIAID, under contract HHSN272200700016I.

Received: May 29, 2015
Revised: July 24, 2015
Accepted: August 11, 2015
Published: September 10, 2015

REFERENCES

Baize, S., Pannetier, D., Oestereich, L., Rieger, T., Koivogui, L., Magassouba, N., Soropogui, B., Sow, M.S., Keïta, S., De Clerck, H., et al. (2014). Emergence of Zaire Ebola virus disease in Guinea. N. Engl. J. Med. *371*, 1418–1425.

Bale, S., Dias, J.M., Fusco, M.L., Hashiguchi, T., Wong, A.C., Liu, T., Keuhne, A.I., Li, S., Woods, V.L., Jr., Chandran, K., et al. (2012). Structural basis for differential neutralization of ebolaviruses. Viruses *4*, 447–470.

Carneiro, M.O., Russ, C., Ross, M.G., Gabriel, S.B., Nusbaum, C., and DePristo, M.A. (2012). Pacific biosciences sequencing technology for genotyping and variation discovery in human data. BMC Genomics *13*, 375.

Carroll, S.A., Towner, J.S., Sealy, T.K., McMullan, L.K., Khristova, M.L., Burt, F.J., Swanepoel, R., Rollin, P.E., and Nichol, S.T. (2013). Molecular evolution of viruses of the family *Filoviridae* based on 97 whole-genome sequences. J. Virol. *87*, 2608–2616.

Chaisson, M.J., and Tesler, G. (2012). Mapping single molecule sequencing reads using basic local alignment with successive refinement (BLASR): application and theory. BMC Bioinformatics *13*, 238.

Dias, J.M., Kuehne, A.I., Abelson, D.M., Bale, S., Wong, A.C., Halfmann, P., Muhammad, M.A., Fusco, M.L., Zak, S.E., Kang, E., et al. (2011). A shared structural solution for neutralizing ebolaviruses. Nat. Struct. Mol. Biol. *18*, 1424–1427.

Excoffier, L., and Lischer, H.E. (2010). Arlequin suite ver 3.5: a new series of programs to perform population genetics analyses under Linux and Windows. Mol. Ecol. Resour. *10*, 564–567.

Feldmann, H., Jones, S.M., Daddario-DiCaprio, K.M., Geisbert, J.B., Ströher, U., Grolla, A., Bray, M., Fritz, E.A., Fernando, L., Feldmann, F., et al. (2007). Effective post-exposure treatment of Ebola infection. PLoS Pathog. *3*, e2.

Geisbert, T.W., Daddario-Dicaprio, K.M., Geisbert, J.B., Reed, D.S., Feldmann, F., Grolla, A., Ströher, U., Fritz, E.A., Hensley, L.E., Jones, S.M., and Feldmann, H. (2008). Vesicular stomatitis virus-based vaccines protect nonhuman primates against aerosol challenge with Ebola and Marburg viruses. Vaccine *26*, 6894–6900.

Geisbert, T.W., Geisbert, J.B., Leung, A., Daddario-DiCaprio, K.M., Hensley, L.E., Grolla, A., and Feldmann, H. (2009). Single-injection vaccine protects nonhuman primates against infection with marburg virus and three species of ebola virus. J. Virol. *83*, 7296–7304.

Geisbert, T.W., Lee, A.C., Robbins, M., Geisbert, J.B., Honko, A.N., Sood, V., Johnson, J.C., de Jong, S., Tavakoli, I., Judge, A., et al. (2010). Postexposure protection of non-human primates against a lethal Ebola virus challenge with RNA interference: a proof-of-concept study. Lancet *375*, 1896–1905.

Iversen, P.L., Warren, T.K., Wells, J.B., Garza, N.L., Mourich, D.V., Welch, L.S., Panchal, R.G., and Bavari, S. (2012). Discovery and early development of AVI-7537 and AVI-7288 for the treatment of Ebola virus and Marburg virus infections. Viruses *4*, 2806–2830.

Kugelman, J.R., Lee, M.S., Rossi, C.A., McCarthy, S.E., Radoshitzky, S.R., Dye, J.M., Hensley, L.E., Honko, A., Kuhn, J.H., Jahrling, P.B., et al. (2012). Ebola virus genome plasticity as a marker of its passaging history: a

comparison of in vitro passaging to non-human primate infection. PLoS ONE *7*, e50316.

Kuhn, J.H. (2008). Filoviruses. A compendium of 40 years of epidemiological, clinical, and laboratory studies. Arch. Virol. Suppl. *20*, 13–360.

Lee, J.E., and Saphire, E.O. (2009). Neutralizing ebolavirus: structural insights into the envelope glycoprotein and antibodies targeted against it. Curr. Opin. Struct. Biol. *19*, 408–417.

Lee, J.E., Fusco, M.L., Hessell, A.J., Oswald, W.B., Burton, D.R., and Saphire, E.O. (2008). Structure of the Ebola virus glycoprotein bound to an antibody from a human survivor. Nature *454*, 177–182.

Maruyama, T., Parren, P.W., Sanchez, A., Rensink, I., Rodriguez, L.L., Khan, A.S., Peters, C.J., and Burton, D.R. (1999). Recombinant human monoclonal antibodies to Ebola virus. J. Infect. Dis. *179* (*Suppl 1*), S235–S239.

McCarthy, M. (2014). US signs contract with ZMapp maker to accelerate development of the Ebola drug. BMJ *349*, g5488.

Olal, D., Kuehne, A.I., Bale, S., Halfmann, P., Hashiguchi, T., Fusco, M.L., Lee, J.E., King, L.B., Kawaoka, Y., Dye, J.M., Jr., and Saphire, E.O. (2012). Structure of an antibody in complex with its mucin domain linear epitope that is protective against Ebola virus. J. Virol. *86*, 2809–2816.

Olinger, G.G., Jr., Pettitt, J., Kim, D., Working, C., Bohorov, O., Bratcher, B., Hiatt, E., Hume, S.D., Johnson, A.K., Morton, J., et al. (2012). Delayed treatment of Ebola virus infection with plant-derived monoclonal antibodies provides protection in rhesus macaques. Proc. Natl. Acad. Sci. USA *109*, 18030–18035.

Ono, Y., Asai, K., and Hamada, M. (2013). PBSIM: PacBio reads simulator–toward accurate genome assembly. Bioinformatics *29*, 119–121.

Penty, C., and Benoit, A. (2014). Spain Deputy Prime Minister Takes Charge of Ebola Effort (Bloomberg News).

Qiu, X., Alimonti, J.B., Melito, P.L., Fernando, L., Ströher, U., and Jones, S.M. (2011). Characterization of Zaire ebolavirus glycoprotein-specific monoclonal antibodies. Clin. Immunol. *141*, 218–227.

Qiu, X., Audet, J., Wong, G., Pillet, S., Bello, A., Cabral, T., Strong, J.E., Plummer, F., Corbett, C.R., Alimonti, J.B., and Kobinger, G.P. (2012a). Successful treatment of ebola virus-infected cynomolgus macaques with monoclonal antibodies. Sci. Transl. Med. *4*, 138ra81.

Qiu, X., Fernando, L., Melito, P.L., Audet, J., Feldmann, H., Kobinger, G., Alimonti, J.B., and Jones, S.M. (2012b). Ebola GP-specific monoclonal antibodies protect mice and guinea pigs from lethal Ebola virus infection. PLoS Negl. Trop. Dis. *6*, e1575.

Qiu, X., Audet, J., Wong, G., Fernando, L., Bello, A., Pillet, S., Alimonti, J.B., and Kobinger, G.P. (2013). Sustained protection against Ebola virus infection following treatment of infected nonhuman primates with ZMAb. Sci. Rep. *3*, 3365.

Qiu, X., Wong, G., Audet, J., Bello, A., Fernando, L., Alimonti, J.B., Fausther-Bovendo, H., Wei, H., Aviles, J., Hiatt, E., et al. (2014a). Reversion of advanced Ebola virus disease in nonhuman primates with ZMapp. Nature *514*, 47–53.

Qiu, X., Wong, G., Audet, J., Bello, A., Fernando, L., Alimonti, J.B., Fausther-Bovendo, H., Wei, H., Aviles, J., Hiatt, E., et al. (2014b). Reversion of advanced Ebola virus disease in nonhuman primates with ZMapp. Nature *514*, 47–53.

Suzuki, Y., and Gojobori, T. (1997). The origin and evolution of Ebola and Marburg viruses. Mol. Biol. Evol. *14*, 800–806.

Takada, A., Robison, C., Goto, H., Sanchez, A., Murti, K.G., Whitt, M.A., and Kawaoka, Y. (1997). A system for functional analysis of Ebola virus glycoprotein. Proc. Natl. Acad. Sci. USA *94*, 14764–14769.

Teacher, A.G., and Griffiths, D.J. (2011). HapStar: automated haplotype network layout and visualization. Mol. Ecol. Resour. *11*, 151–153.

Volchkova, V.A., Dolnik, O., Martinez, M.J., Reynard, O., and Volchkov, V.E. (2011). Genomic RNA editing and its impact on Ebola virus adaptation during serial passages in cell culture and infection of guinea pigs. J. Infect. Dis. *204* (*Suppl 3*), S941–S946.

Warfield, K.L., Swenson, D.L., Olinger, G.G., Nichols, D.K., Pratt, W.D., Blouch, R., Stein, D.A., Aman, M.J., Iversen, P.L., and Bavari, S. (2006). Gene-specific countermeasures against Ebola virus based on antisense phosphorodiamidate morpholino oligomers. PLoS Pathog. *2*, e1.

Warren, T.K., Warfield, K.L., Wells, J., Swenson, D.L., Donner, K.S., Van Tongeren, S.A., Garza, N.L., Dong, L., Mourich, D.V., Crumley, S., et al. (2010). Advanced antisense therapies for postexposure protection against lethal filovirus infections. Nat. Med. *16*, 991–994.

WHO (2014a). Ethical Considerations for Use of Unregistered Interventions for Ebola Virus Disease (EVD) (World Health Organization).

WHO (2014b). Global Alert and Response (GAR) - Ebola Virus Disease (EVD) (World Health Organization).

WHO (2015) Ebola Situation Report - 11 March 2015. http://apps.who.int/ebola/current-situation/ebola-situation-report-11-march-2015.

Wilson, J.A., Hevey, M., Bakken, R., Guest, S., Bray, M., Schmaljohn, A.L., and Hart, M.K. (2000). Epitopes involved in antibody-mediated protection from Ebola virus. Science *287*, 1664–1666.